

# Hole mobility of $p$ -type $\beta$ -FeSi<sub>2</sub> thin films grown from Si/Fe multilayers

K. Takakura and H. Ohyama

*Kumamoto National College of Technology, 2659-2 Suya, Nishigoshi, Kikuchi, Kumamoto 861-1102, Japan*

K. Takarabe

*Okayama University of Science, Ridai, Okayama City, Okayama 700-0005, Japan*

T. Suemasu<sup>a)</sup>

*Institute of Applied Physics, University of Tsukuba, 1-1-1 Tenmodai, Tsukuba, Ibaraki 305-8573, Japan*

F. Hasegawa

*Department of Electronic Engineering, Kogakuin University, 2665-1 Nakano, Hachioji, Tokyo 192-0005, Japan*

(Received 29 November 2004; accepted 22 February 2005; published online 22 April 2005)

The hole mobility of intentionally undoped  $p$ -type  $\beta$ -FeSi<sub>2</sub> thin films grown by a multilayer method was investigated. With increasing annealing temperature and time, the hole mobility increased to approximately 450 cm<sup>2</sup>/V s at room temperature (RT). The observed hole mobility was analyzed by considering various carrier scatterings such as acoustic-phonon and polar-optical-phonon scatterings, intervalley scattering, ionized impurity scattering, and grain-boundary scattering. The nice fit of the mobility to the experimental results reveals that the polar-optical-phonon scattering determines the hole mobility at RT. © 2005 American Institute of Physics.

[DOI: 10.1063/1.1891279]

## I. INTRODUCTION

$\beta$ -FeSi<sub>2</sub> has been attracting significant attention due to its large absorption coefficient of over 10<sup>5</sup> cm<sup>-1</sup> at 1 eV.<sup>1</sup> Recent reports on light-emitting diodes operating at the wavelength corresponding to optical fiber communication (~1.5  $\mu$ m) have renewed interest in  $\beta$ -FeSi<sub>2</sub>.<sup>2,3</sup> Therefore,  $\beta$ -FeSi<sub>2</sub> is considered to be promising as an infrared light emitter and a detector on Si substrates. In the past decade, a number of growth methods have been attempted for the fabrication of  $\beta$ -FeSi<sub>2</sub> films. However, the electron and hole mobilities for  $\beta$ -FeSi<sub>2</sub> have been relatively low in all these cases, typically on the order of several tens of cm<sup>2</sup>/V s at room temperature (RT). In an earlier study, we were able to obtain a hole mobility of  $\mu_p=13\,000$  cm<sup>2</sup>/V s at 50 K ( $\mu_p=450$  cm<sup>2</sup>/V s at RT) by high-temperature (900 °C) and long-time (14 h) annealing of highly [100]-oriented  $p$ -type  $\beta$ -FeSi<sub>2</sub> films grown from Si/Fe multilayers using templates and a SiO<sub>2</sub> capping layer.<sup>4</sup> However, the scattering mechanisms affecting the measured mobility have not been clarified. Furthermore, the highest mobility that could be obtained in  $\beta$ -FeSi<sub>2</sub> at RT, which is very important for device applications, has not been clarified.

The purpose of the present work is to analyze the temperature dependence of hole mobility in this high-quality  $\beta$ -FeSi<sub>2</sub> film and to elucidate carrier scattering mechanisms in  $\beta$ -FeSi<sub>2</sub>.

## II. EXPERIMENTAL METHODS

An ion-pumped molecular-beam epitaxy (MBE) system equipped with electron gun evaporation sources for Si and Fe was used in this study.  $N$ -type floating-zone Si (001) sub-

strates with resistivity higher than 3000  $\Omega$  cm was used. The growth procedure for highly [100]-oriented  $\beta$ -FeSi<sub>2</sub> films has been described in a previous report.<sup>5</sup> Firstly, a 20-nm-thick  $\beta$ -FeSi<sub>2</sub> template was grown at 470 °C by reactive deposition epitaxy (RDE),<sup>6</sup> that is Fe deposition on a hot Si substrate. Fe deposition rate was 0.6 nm/min.<sup>7</sup> The template layer was grown in order to control the crystal orientation of the  $\beta$ -FeSi<sub>2</sub> film.<sup>8</sup> Forty-two periods of the Si(1.6 nm)/Fe(0.6 nm) multilayers corresponding to a 90-nm-thick  $\beta$ -FeSi<sub>2</sub> film including the template were then deposited. The deposited Si/Fe atomic ratio was approximately 1.6. After the deposition, the wafers were transferred to another vacuum chamber to cover the multilayers with an approximately 100-nm-thick SiO<sub>2</sub> capping layer by electron-beam evaporation of SiO<sub>2</sub> pellets. The wafers were then annealed in an Ar atmosphere at 800 °C for 3 h to form a continuous  $\beta$ -FeSi<sub>2</sub> film. The samples were further annealed at 900 °C for 1 or 14 h in order to improve the crystalline quality of  $\beta$ -FeSi<sub>2</sub>. The SiO<sub>2</sub> capping layer prevents aggregation of the  $\beta$ -FeSi<sub>2</sub> film into islands.<sup>8</sup> Samples were prepared as summarized in Table I. The ohmic contacts were formed on the  $\beta$ -FeSi<sub>2</sub> film after removal of the SiO<sub>2</sub> capping layer using buffered HF solution (HF:NH<sub>4</sub>F=1:45). The hole density and mobility were measured at tempera-

TABLE I. Sample preparation conditions. Thickness of  $\beta$ -FeSi<sub>2</sub>, and the annealing conditions are listed for the three samples used.

Sample	$\beta$ -FeSi <sub>2</sub> film (nm)	Formation of $\beta$ -FeSi <sub>2</sub>	Annealing
A	90	800 °C/3 h	no
B	90	800 °C/3 h	900 °C/1 h
C	90	800 °C/3 h	900 °C/14 h

<sup>a)</sup>Electronic mail: suemasu@bk.tsukuba.ac.jp

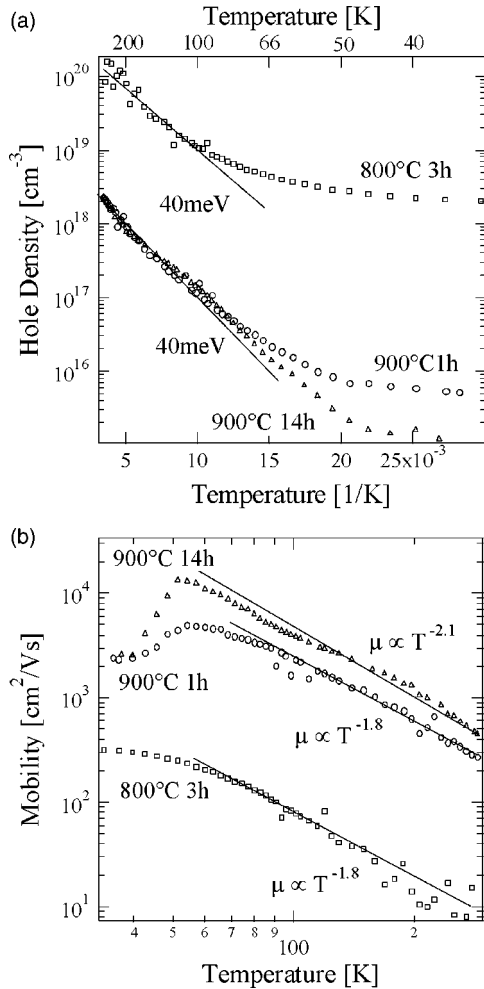


FIG. 1. Temperature dependence of (a) hole density and (b) hole mobility of the  $\beta$ -FeSi<sub>2</sub> films prepared under different annealing conditions.

tures between 30 and 300 K using the Van der Pauw method. The applied magnetic field was 0.2 T normal to the sample surface.

### III. RESULTS AND DISCUSSION

The temperature dependence of the hole density and the hole mobility of these differently annealed samples is shown in Figs. 1(a) and 1(b). All the samples showed  $p$ -type conduction. It has been reported that the conduction-type in undoped  $\beta$ -FeSi<sub>2</sub> depends on the deposited Si/Fe ratio.<sup>4,9–11</sup> We found that the  $\beta$ -FeSi<sub>2</sub> films with the deposited Si/Fe atomic ratios of 1.9 and 2.0 exhibited  $n$ -type conduction, whereas those with 1.5–1.8 exhibited  $p$ -type conduction.<sup>4,11</sup> Electron-paramagnetic-resonance (EPR) measurements of undoped  $n$ - and  $p$ -type  $\beta$ -FeSi<sub>2</sub> showed that the Fe and Si vacancies in  $\beta$ -FeSi<sub>2</sub> act as donors and acceptors, respectively.<sup>12,13</sup> Here, the influence of the  $n$ -type Si substrate on the measured Hall voltages should be considered. The sheet resistance of the Si substrate was higher than  $10^7 \Omega$ .<sup>10</sup> This value was approximately two orders of magnitude larger than that of the  $\beta$ -FeSi<sub>2</sub>/Si sample over the entire temperature range measured in this work. Therefore, it is safely expected that the substrate effect is negligible.

When the annealing temperature was raised from 800 to 900 °C, the hole density decreased and the hole mobility increased. A maximum mobility of 13 000 cm<sup>2</sup>/V s was obtained at 50 K for sample C. From Fig. 1(b), the  $n$  values, obtained assuming that the mobility varies with  $1/T^n$  at high temperatures, changed from  $n=1.8$  to  $n=2.1$ . This shows that the mobility could not be explained only by acoustic-phonon scattering ( $n=1.5$ ). Therefore, the other scattering mechanisms such as polar-optical-phonon, intervalley, and ionized impurity scatterings<sup>14</sup> should be properly considered in order to explain the measured high mobility shown in Fig. 1(b). Grain-boundary scattering was found to be important in this  $\beta$ -FeSi<sub>2</sub> film, as will be described later.

The mobilities from acoustic-phonon scattering  $\mu_{ac}$  and nonpolar optical-phonon scattering  $\mu_{po}$  are, respectively, given by<sup>14</sup>

$$\mu_{ac} = 9.36 \times 10^3 \frac{\rho u_l^2}{(m^*/m_0)^{2.5} E_{ac}^2} \frac{1}{T^{1.5}} \quad (1)$$

and

$$\mu_{po} = 25.4 \frac{T^{0.5}}{\theta (m^*/m_0)^{1.5}} \left( \frac{1}{\epsilon_\infty} - \frac{1}{\epsilon_0} \right) (e^{\theta/T} - 1) \times \left( 0.4 + \frac{0.148\theta}{T} \right), \quad (2)$$

where  $\rho$  is the density of  $\beta$ -FeSi<sub>2</sub> (4.93 g/cm<sup>3</sup>),  $u_l$  the sound velocity,  $m^*$  the effective mass of hole,  $m_0$  the free-electron mass,  $E_{ac}$  the deformation potential of acoustic phonon,  $T$  the temperature,  $\theta$  the Debye temperature, and  $\epsilon_\infty$  and  $\epsilon_0$  the high-frequency and the dc dielectric constants, respectively. The sound velocity  $u_l$  is given by<sup>14</sup>

$$u_l \cong \frac{2\pi k_B \theta}{h} \left( \frac{V/48}{6\pi^2} \right)^{1/3}, \quad (3)$$

where  $k_B$  is the Boltzmann's constant,  $h$  the Planck's constant, and  $V$  the volume of the unit cell.  $m^*$  of  $\beta$ -FeSi<sub>2</sub> is reported to be between  $0.6m_0$  and  $1.0m_0$ , and thus the value of  $m^*/m_0=0.75$  is used in the analysis. The dielectric constants are  $\epsilon_0=29.9$  and  $\epsilon_\infty=9.89$ , respectively.<sup>15</sup>

The valence-band maximum for  $\beta$ -FeSi<sub>2</sub> is not located at the center of the Brillouin zone, but at the  $Y$  point ( $\pm 2\pi/a, 0, 0$ ), known from first-principles band-structure calculations.<sup>16</sup> Therefore, the intervalley scattering among the  $Y$  points is also taken into account. The mobility determined by intervalley scattering involving acoustic phonon  $\mu_{ac,v}$  is given by<sup>14</sup>

$$\mu_{ac,v} = \mu_{ac} \left[ 1 + \frac{4w \theta_v^2 K_1(\theta_v/2T)}{3\pi T^2 \sinh(\theta_v/2T)} \right], \quad (4)$$

where  $w$  is the constant,  $\theta_v$  the temperature converted from intervalley phonon energy, and  $K_1$  the modified Bessel functions of the second kind.

The mobility from ionized impurities  $\mu_i$  is described by<sup>14</sup>

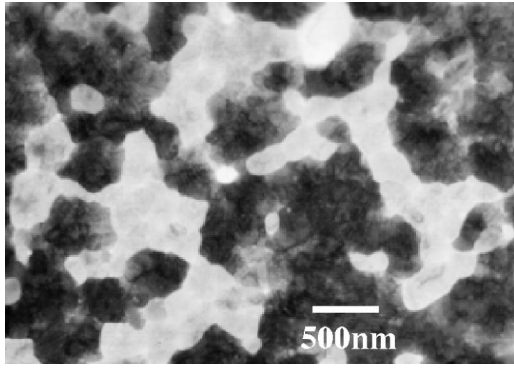


FIG. 2. Plan-view TEM micrograph of the  $\beta$ -FeSi<sub>2</sub> film (sample C) obtained along the [001] azimuth of Si.

$$\mu_i = \frac{2^{3.5}(4\pi\epsilon_0)^2(k_B T)^{1.5}}{\pi^{1.5}q^3(m^*m_0)^{0.5}N_i[\ln(1 + \beta_{BH}^2) - \beta_{BH}^2/(1 + \beta_{BH}^2)]}. \quad (5)$$

The parameter  $\beta_{BH}$  was given by Brooks and Herring as

$$\beta_{BH} = \frac{2m^*}{\hbar} \left( \frac{2}{m^*} 3k_B T \right)^{0.5} L_D, \quad (6)$$

where  $L_D$  is the Debye length. These elastic mobility scatterings are described in detail in Ref. 14.

The fit to the experimental results obtained by solely using the above scatterings is not satisfactory. Thus, other scattering mechanisms also affect the actual mobility, in addition to the ones discussed above. Figure 2 shows the plan-view transmission electron microscopy (TEM) photograph of sample C, which was taken along the [001] azimuth of Si. Many grains of approximately 100-nm size are seen. It was found from electron-diffraction analysis that the black parts correspond to  $\beta$ -FeSi<sub>2</sub> with orientation alignment of  $\beta$ -FeSi<sub>2</sub>(100)//Si(001) with  $\beta$ -FeSi<sub>2</sub>[010]//Si[110] and  $\beta$ -FeSi<sub>2</sub>[001]//Si[110], while the white parts correspond to that of either  $\beta$ -FeSi<sub>2</sub>(110)//Si(001) with  $\beta$ -FeSi<sub>2</sub>[001]//Si[110] or  $\beta$ -FeSi<sub>2</sub>(101)//Si(001) with  $\beta$ -FeSi<sub>2</sub>[010]//Si[110]. The presence of grain boundaries results in carrier scattering, and thus grain-boundary scattering needs to be considered in the analysis. Tarnag has studied grain-boundary scattering in polycrystalline silicon films.<sup>17</sup> On the basis of his report, if there are a large number of carrier trap centers at the grain boundaries, these centers may capture carriers and thus introduce band bending and an energy barrier at the grain boundary. The energy barrier at the grain boundary reduces the mobility of carriers. However, the carriers can tunnel the barrier by thermionic field emission (TFE), wherein the barrier height is lowered below the true barrier because the effective tunneling length is determined both by the shape of the barrier and the thermal distribution of the carriers. The mobility from the grain boundaries  $\mu_g$  with TFE is given by<sup>17</sup>

$$\mu_g = \frac{A^* L}{k_B p'} T \exp\left(-\frac{q\phi_{\text{eff}}}{k_B T}\right), \quad (7)$$

where  $A^*$  is the Richardson constant,  $L$  the grain size,  $p'$  the mean hole density, and  $\phi_{\text{eff}}$  the effective barrier height at the

grain boundaries being temperature dependent.  $A^*$  can be determined using the following:<sup>18</sup>

$$A^* = \frac{4\pi q m^* k_B^2}{h^3}. \quad (8)$$

We also considered the mean hole density  $p'$  as follows. The hole density decreases around the grain boundaries because of band bending. If the space charges are uniformly distributed in the bulk, the barrier height is assumed to be expressed as

$$\phi(x) = \frac{\phi_B}{(L/2)^2} \left(x - \frac{L}{2}\right)^2 \quad \left(0 \leq x \leq \frac{L}{2}\right) \quad (9a)$$

and

$$\phi(x) = \frac{\phi_B}{(L/2)^2} \left(-x - \frac{L}{2}\right)^2 \quad \left(-\frac{L}{2} \leq x \leq 0\right), \quad (9b)$$

where  $x$  is the distance from the grain boundary,  $\phi_B$  the maximum barrier height at the grain boundary, and  $L$  the grain size. Therefore,  $p'$  is given by the following integration.

$$p' = \left[ \int_{-L/2}^{L/2} p \exp\left(-\frac{q\phi(x)}{k_B T}\right) dx \right] / L. \quad (10)$$

Substituting Eq. (10) into Eqs. (9a) and (9b) yields

$$p' = p \sqrt{\frac{k_B T}{q\phi_{\text{eff}}}} \frac{\pi^{0.5}}{2} \left(1 - \exp\left[-2\left(\frac{q\phi_{\text{eff}}}{k_B T}\right)\right]\right). \quad (11)$$

Here,  $\phi_B$  is replaced with the  $\phi_{\text{eff}}$ .

The total mobility, as a function of temperature, is then given by Mathiessen's rule as

$$\mu_{\text{tot}}^{-1} = \mu_{\text{ac},v}^{-1} + \mu_{\text{po}}^{-1} + \mu_i^{-1} + \mu_g^{-1}. \quad (12)$$

Figures 3(a)–3(c) show the calculated hole mobilities using Eq. (12) and the measured ones ( $\bullet$ ) for the three samples A, B, and C, respectively, where  $\mu_{\text{ac},v}$  and  $\mu_{\text{po}}$  are calculated using the same parameter values for the three samples since they are intrinsic. In contrast,  $\mu_i$  and  $\mu_g$  are extrinsic so that the parameter values can be changed to fit the experimental hole mobilities.

The parameters used in the fit are summarized in Table II. The deformation potential of acoustic phonons  $E_{\text{ac}}$  is 0.5 eV. This value is smaller than 1 eV which is the usual value for semiconductors such as Si and GaAs. However, according to van de Walle,<sup>19</sup>  $E_{\text{ac}}$  was determined to be 0.36 eV for InSb and 0.55 eV for CdTe. A smaller value of  $E_{\text{ac}}$  was also reported by Wei and Zunger.<sup>20</sup>  $\theta$  is taken from the report of Arushanov *et al.*<sup>21</sup>  $\epsilon_0$  is almost the same as that reported in Ref. 15.  $\epsilon_{\infty}$  is, however, approximately double the reported value of 9.89. The polar-phonon scattering becomes too small to explain the experimental result if  $\epsilon_{\infty}$  is taken to be 9.89. The fit shows that a value of 23 for  $\epsilon_{\infty}$  reproduces the temperature dependence of mobility very well. According to recent reflectivity measurements by Uono *et al.*, the low-frequency dielectric constant was reported to be around 25.<sup>22</sup>  $\mu_{\text{ac},v}$  is smaller than  $\mu_{\text{ac}}$  over the entire temperature range, as shown by the dotted lines in Fig. 3. This reduction is gov-

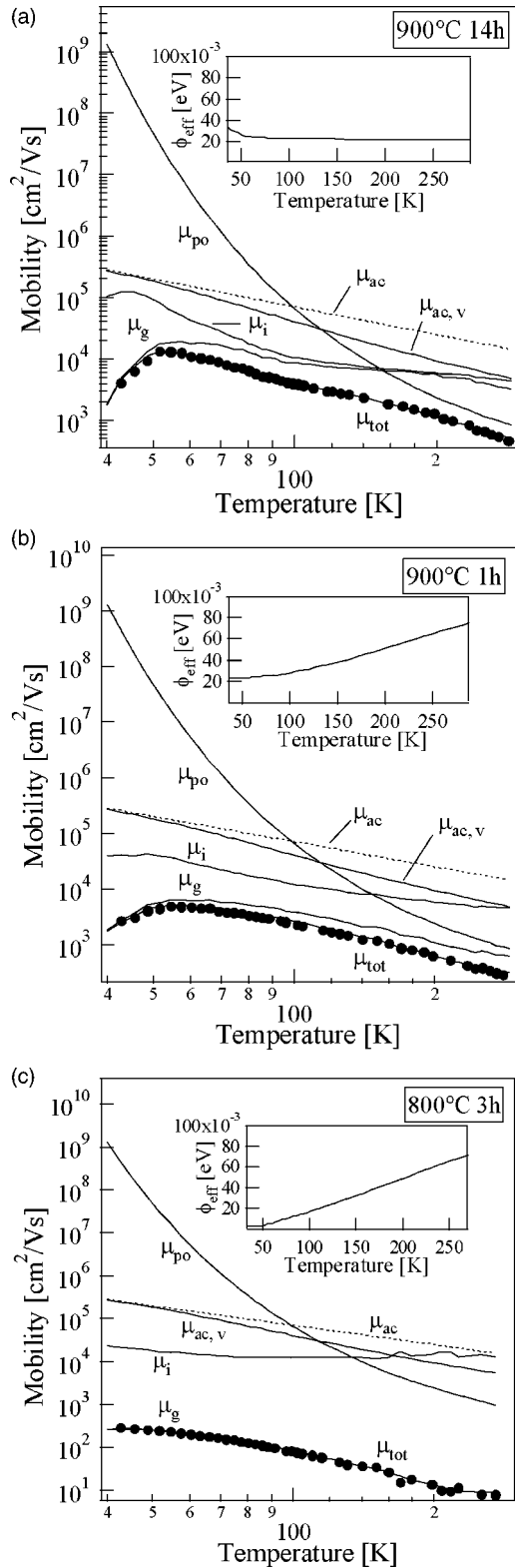


FIG. 3. Temperature dependence of calculated and measured mobilities of  $\beta$ -FeSi<sub>2</sub> obtained for (a) sample C, (b) sample B, and (c) sample A. The data points indicate experimental values.

TABLE II. Parameters used in the fit.

Parameter	$E_{ac}$	$\theta$	$m^*/m_0$	$\theta_v$	$\epsilon_0$	$\epsilon_\infty$	$w$
Value	0.5 eV	640 K	0.75	300 K	28	23	1.5

erned by the value of  $w$  used in Eq. (4). In Si, it was reported that the mobility can be reproduced well at temperatures higher than RT when  $w$  is 3.<sup>14</sup> The energy of intervalley scattering ( $k_B\theta_v=26$  meV) takes a medium value between optical- and acoustic-phonon energies. The optical-phonon energy is known as  $k_B\theta=56$  meV,<sup>21</sup> but the acoustic-phonon energy is not known. The TFE probability changes with temperature, that is the effective tunneling barrier height depends on temperature. The temperature dependence of the effective tunneling barrier height for each fit is shown in the insets of Figs. 3(a)–3(c). These characteristic changes are not yet understood.

The grain sizes used for the fit are 50, 50, and 100 nm for samples A, B, and C, respectively. The measured mobilities are surprisingly reproduced well by Eq. (12) for all the annealing conditions. It is known that the mobility obtained for sample A, after annealing at 800 °C for 3 h, is limited by grain-boundary scattering, as shown in Fig. 3(c), where  $L$  is taken to be 50 nm. There is no TEM photograph for samples A and B, but the grain size of these two samples is reasonably assumed to be smaller than that for sample C. The TEM micrograph for sample C (Fig. 2) shows that  $L$  is approximately 1000 nm in one direction, but about 100 nm in another direction. The carrier scattering is determined effectively by the shorter grain size. Thus,  $L=50$  nm for sample A is considered to be a reasonable value. In the case of sample C, which was obtained after an additional 900 °C annealing of sample A for 14 h, the grain-boundary scattering limits the mobility at low temperatures but the polar-optical-phonon scattering becomes dominant at RT, as shown in Fig. 3(a). Very recently, Tassis *et al.* have also reported that the polar-optical-phonon scattering is probable in  $\beta$ -FeSi<sub>2</sub> thin films at high temperatures.<sup>23</sup>

It was found from the above analysis that the decrease in mobility at high temperature is particularly important in order to consider intervalley scattering or the fact that the  $\mu_{ac,v}$  is smaller than the  $\mu_{ac}$  in the high-temperature region. On the other hand, it is reasonable to include the intervalley scattering from the viewpoint of the band structure of  $\beta$ -FeSi<sub>2</sub>. Consequently the decrease in the mobility at high temperature is partly due to the intervalley scattering. If the extrinsic scatterings such as grain-boundary scattering or impurity scattering are removed and the acoustic-phonon scattering dominates the mobility at low temperature, it can be safely expected that the hole mobility can reach 270 000 cm<sup>2</sup>/V s at 40 K and 800 cm<sup>2</sup>/V s at RT. Thus  $p$ -type  $\beta$ -FeSi<sub>2</sub> can be considered to be very promising for various device applications.

#### IV. SUMMARY

The temperature dependence of the hole mobility of continuous  $\beta$ -FeSi<sub>2</sub> films grown using a multilayer method is

investigated. The analysis showed that the temperature dependence of the hole mobility is well reproduced by taking into account several scattering mechanisms such as acoustic- and polar-optical-phonon scatterings, the intervalley scattering, ionized impurity scattering, and grain-boundary scattering. The hole mobility of the  $\beta$ -FeSi<sub>2</sub> film obtained after annealing at 800 °C for 3 h is limited by the grain-boundary scattering. In contrast, the mobility increased almost up to the intrinsic value of  $\beta$ -FeSi<sub>2</sub> and is dominated by polar-optical-phonon scattering at room temperature for the sample annealed at 900 °C for 14 h.

## ACKNOWLEDGMENT

The author would like to express thanks to Professor K. Tatsuoka of the Shizuoka University for his help in TEM observations.

<sup>1</sup>M. C. Bost and J. E. Mahan, *J. Appl. Phys.* **64**, 2034 (1988).

<sup>2</sup>D. Leong, M. Harry, K. J. Reeson, and K. P. Homewood, *Nature (London)* **387**, 686 (1997).

<sup>3</sup>T. Suemasu, Y. Negishi, K. Takakura, and F. Hasegawa, *Jpn. J. Appl. Phys., Part 2* **39**, L1013 (2000).

<sup>4</sup>K. Takakura, T. Suemasu, Y. Ikura, and F. Hasegawa, *Jpn. J. Appl. Phys., Part 2* **39**, L789 (2000).

<sup>5</sup>K. Takakura, T. Suemasu, N. Hiroi, and F. Hasegawa, *Jpn. J. Appl. Phys., Part 2* **39**, L233 (2000).

<sup>6</sup>J. E. Mahan, K. M. Geib, G. Y. Robinson, R. G. Long, X. Yan, G. Bai, M. A. Nicolet, and M. Nathan, *Appl. Phys. Lett.* **56**, 2126 (1990).

<sup>7</sup>M. Tanaka, Y. Kumagai, T. Takakura, and F. Hasegawa, *Jpn. J. Appl. Phys., Part 1* **36**, 3620 (1997).

<sup>8</sup>T. Suemasu, N. Hiroi, T. Fujii, K. Takakura, and F. Hasegawa, *Jpn. J. Appl. Phys., Part 2* **38**, L878 (1999).

<sup>9</sup>J. Tani and H. Kido, *J. Appl. Phys.* **84**, 1408 (1998).

<sup>10</sup>K. Takakura, T. Suemasu, and F. Hasegawa, *Jpn. J. Appl. Phys., Part 2* **40**, L249 (2001).

<sup>11</sup>T. Suemasu, K. Takakura, C. Li, Y. Ozawa, Y. Kumagai, and F. Hasegawa, *Thin Solid Films* **461**, 209 (2004).

<sup>12</sup>T. Miki, Y. Matsui, Y. Teraoka, Y. Ebina, K. Matsubara, and K. Kishimoto, *J. Appl. Phys.* **76**, 2097 (1994).

<sup>13</sup>I. Aksenov, H. Katsumata, Y. Makita, Y. Kimura, T. Shinzato, and K. Sato, *J. Appl. Phys.* **80**, 1678 (1996).

<sup>14</sup>K. Seeger, *Semiconductor Physics* (Springer, Heidelberg, 1989).

<sup>15</sup>H. Kakemoto, Y. Makita, S. Sakuragi, and T. Tsukamoto, *Jpn. J. Appl. Phys., Part 1* **38**, 5192 (1999).

<sup>16</sup>L. Miglio, V. Merefalli, and O. Jepsen, *Appl. Phys. Lett.* **75**, 385 (1999).

<sup>17</sup>M. L. Tarng, *J. Appl. Phys.* **49**, 4069 (1978).

<sup>18</sup>S. M. Sze, *Physics of Semiconductor Devices*, 2nd ed. (Wiley, New York, 1981).

<sup>19</sup>C. G. van de Walle, *Phys. Rev. B* **39**, 1871 (1989).

<sup>20</sup>S.-H. Wei and A. Zunger, *Phys. Rev. B* **60**, 5404 (1999).

<sup>21</sup>E. Arushanov, H. Lange, and J. Werner, *Phys. Status Solidi A* **166**, 853 (1998).

<sup>22</sup>H. Udono, I. Kikuma, T. Okuno, Y. Masumoto, H. Tajima, and S. Komuro, *Thin Solid Films* **46**, 182 (2004).

<sup>23</sup>D. H. Tassis, D. Evangelinos, O. Valassiades, and C. A. Dimitriadis, *J. Appl. Phys.* **96**, 6504 (2004).